

# <sup>31</sup>P NMR Studies of Enzyme-Bound Substrate Complexes of Yeast 3-Phosphoglycerate Kinase. 1. Effects of Sulfate and pH. Mg(II) Affinity at the Two ATP Sites<sup>†</sup>

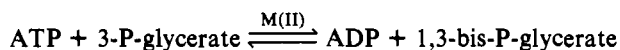
Bruce D. Ray and B. D. Nageswara Rao\*

Department of Physics, Indiana University—Purdue University at Indianapolis (IUPUI), P.O. Box 647, Indianapolis, Indiana 46223

Received November 10, 1987; Revised Manuscript Received March 1, 1988

**ABSTRACT:** <sup>31</sup>P NMR measurements were made (at 121.5 MHz and 5 °C) on enzyme-bound substrate complexes of 3-phosphoglycerate kinase in order to address three questions pertaining to (i) the integrity of the enzyme-substrate complexes with Mg(II) in the presence of sulfate concentrations typical of those used for crystallization in X-ray studies, (ii) the relative affinities of Mg(II) to ATP bound at the two sites on the enzyme, and (iii) the pH behavior of the different phosphate groups in the enzyme complexes. <sup>31</sup>P chemical shift and spin-spin coupling constant changes showed that at concentrations of 0.5 M and higher, sulfate ion interferes with Mg(II) chelation to ATP and ADP free in solution as well as in their enzyme-bound complexes. The effect on enzyme complexes is stronger for the E-MgATP complex than for the E-MgADP complex. Sulfate ion (50 mM) also causes a ~0.5 ppm upfield chemical shift of the <sup>31</sup>P resonance of enzyme-bound 3-P-glycerate even in the absence of ATP or Mg(II). A quantitative estimate of the disparate affinities of Mg(II) to ATP bound at the two sites on the enzyme was made on the basis of computer simulation of changes in the line shape of β-P (ATP) resonance and of changes in <sup>31</sup>P chemical shift of the corresponding γ-P (ATP) in the E-ATP complex with increasing [Mg(II)]. The concentrations of the relevant species that contribute to these <sup>31</sup>P NMR signals were computed by assuming independent binding at the two sites. Detailed comparison between computed and observed spectra yielded the following dissociation constants for ATP and MgATP, respectively, at the two sites: catalytic site, 70 and 65 μM; secondary site, 0.5 and 5.0 mM. <sup>31</sup>P chemical shifts for the enzyme-bound substrates ATP, ADP, and 3-P-glycerate were unaffected by pH in the range 6.4–9.0, whereas these substrates in free solution titrate with pK<sub>a</sub>'s in this range, indicating that in the enzyme complexes these phosphate groups were well sequestered from the bulk solution.

The enzyme 3-phosphoglycerate kinase (ATP:3-phospho-D-glycerate 1-phosphotransferase, EC 2.7.2.3) catalyzes the first ATP<sup>1</sup>-generating reaction in anaerobic glycolysis (Scopes, 1973).



M(II) denotes the obligatory divalent cation for the reaction and is Mg(II) in vivo. The enzyme from yeast, as well as from a variety of other sources, is a single polypeptide chain with a molecular weight of approximately 47 000. X-ray structural data obtained for the enzyme from horse muscle (Banks et al., 1979; Blake & Rice, 1981; Rice & Blake, 1984) and yeast (Bryant et al., 1974; Watson et al., 1982) suggest that the catalytic site spans two globular domains which come together during the reaction. This hinge-bending hypothesis is supported by hydrodynamic (Roustan et al., 1980) and low-angle X-ray scattering measurements (Pickover et al., 1979) and is the subject of recent investigations by biochemical (Adams et al., 1985; Adams & Pain, 1986) and structural techniques (Scheffler & Cohn, 1986) as well as by site-directed mutagenesis (Wilson et al., 1987; Mas et al., 1987). Stereochemical

configuration of MnADP at the active site was probed by EPR methods (Moore & Reed, 1985). Since the amino acid residues of both domains participate in binding the reactants and products, an understanding of the role of the two domains and their mutual interaction in catalysis hinges on knowledge regarding enzyme-substrate interactions.

<sup>31</sup>P NMR offers a convenient method for the study of the interactions of the substrates with this enzyme, since the four substrates contain a total of eight phosphate groups with at least one group on each of them. Previous results obtained by this method (Nageswara Rao et al., 1978) on the yeast enzyme showed that (i) the equilibrium constant for enzyme-bound reactants and products is of the order of unity, in contrast with the catalytic equilibrium constant of ~3000 in favor of ATP production; (ii) there are two ATP molecules bound to the enzyme, one of which, presumably bound at a noncatalytic site, has a significantly weaker affinity for Mg(II) compared to the other, and (iii) the interconversion of the enzyme-bound reactant and products is altered in the presence of sulfate ion.

In this paper, results of <sup>31</sup>P NMR experiments performed to examine in some detail the last two points mentioned above, viz., the effect of the sulfate ion on the interaction of substrates with yeast 3-P-glycerate kinase and the affinity of Mg(II) to ATP bound at the two sites on the enzyme, are presented.

<sup>†</sup>This work was supported in part by grants from NSF (DMB 83 09120 and 86 08185). The NTC-300 NMR spectrometer at IUPUI was purchased with partial support from NSF (PCM 80 18725). A preliminary version of some of this work was presented at the joint meeting of the American Society for Biological Chemists and the Division of Biological Chemistry of the American Chemical Society in Washington, DC, in June 1986.

\* Author to whom correspondence should be addressed.

<sup>1</sup> Abbreviations: ADP, adenosine 5'-diphosphate; ATP, adenosine 5'-triphosphate; HEPES, N-(2-hydroxyethyl)piperazine-N'-2-ethanesulfonic acid; EDTA, ethylenediaminetetraacetic acid; NMR, nuclear magnetic resonance; EPR, electron paramagnetic resonance.

These results are of particular relevance to the design and analysis of  $^{31}\text{P}$  relaxation measurements in the presence of substituent paramagnetic cations to determine the structure of various enzyme-substrate complexes, presented in the following paper (Ray & Nageswara Rao, 1988). Because ammonium sulfate is commonly used in enzyme crystallization for X-ray crystallography, the effects of sulfate on substrate and metal binding in 3-P-glycerate kinase are of crucial importance in comparing previously published crystallographic data (Bryant et al., 1974; Watson et al., 1982) with NMR results. In addition, the pH dependences of  $^{31}\text{P}$  chemical shifts of enzyme-bound ATP, ADP, and 3-P-glycerate are measured and compared with corresponding titrations of these substrates free in solution.

#### EXPERIMENTAL PROCEDURES

**Materials.** ADP, ATP, 3-P-D-glycerate, 1 M  $\text{MgCl}_2$  solution in 0.01 M HCl, and glyceraldehyde-3-phosphate dehydrogenase from yeast were purchased from Sigma Chemical Co. HEPES was obtained from Research Organics, Inc. All other chemicals were of analytical reagent grade. ADP, ATP, 3-P-glycerate, and buffer solutions were passed through a Chelex-100 column before use in the NMR experiments.

**Enzyme Preparation.** 3-P-glycerate kinase was isolated from yeast by the method of Scopes (1971) with the modifications given by Fifis and Scopes (1978). Yeast 3-P-glycerate kinase prepared in this way is sufficiently pure not to require further purification by gel filtration (Fifis & Scopes, 1978). Final protein recrystallization was then done from a solution in 200 mM K-HEPES buffer (pH 8.2). Purified enzyme had a specific activity of  $\sim 1000$  units/mg at  $30^\circ\text{C}$  in a coupled assay system with glyceraldehyde-3-phosphate dehydrogenase (Scopes, 1969). Incubation of 3 mM ATP (or ADP) with 5 mM enzyme for  $\sim 8$  h at  $5^\circ\text{C}$  did not show any hydrolysis in the presence of saturating  $\text{Mg(II)}$ .

Crystalline enzyme was collected by centrifugation at  $20000g$  for 30 min, dissolved in 200 mM K-HEPES buffer (pH 8.2), and dialyzed extensively against the same buffer containing preequilibrated Chelex-100. Enzyme was concentrated up to 220–300 mg/mL by vacuum filtration in a MPDC-120 Micro-ProDiCon concentrator with PA-10 membrane and a tip of volume 1 mL (Biomolecular Dynamics). Protein and nucleotide concentrations were determined spectrophotometrically with  $\epsilon_{280}^{\text{mg/mL}} = 0.490\text{ cm}^{-1}$  and a molecular weight of 47 000 (Scopes, 1973) for the enzyme and  $\epsilon_{259}^{\text{mM}} = 15.4\text{ cm}^{-1}$  for ATP and ADP. A Beckman Altex Model 3500 digital pH meter was used for pH measurements.

**NMR Measurements.**  $^{31}\text{P}$  NMR measurements at 121.5 MHz were made on an NTC-300 wide-bore NMR spectrometer equipped with a 12-mm multinuclear probe, a 293C pulse programmer, a Nicolet 1280 computer, and a variable-temperature controller. A typical sample contained  $\sim 0.8$  mL of the enzyme in an 8-mm o.d. NMR sample tube placed inside a 12-mm NMR tube.  $\text{D}_2\text{O}$  for field-frequency lock was added between the two tubes. Chemical shift measurements were made by using a standard one-pulse sequence with a  $70^\circ$  pulse and taking the  $\beta$ -P of an external standard of 5 mM ATP in 10 mM EDTA and 0.2 M HEPES buffer, pH 8.2, as being at  $-21.5$  ppm.

#### RESULTS

**Effects of Sulfate on Free and Enzyme-Bound  $\text{Mg(II)}$ -Nucleotide Complexes.** Figure 1 shows the effect of varying sulfate concentration on  $^{31}\text{P}$  chemical shifts of  $\text{MgATP}$  free in solution (at  $20^\circ\text{C}$ ) and bound to 3-P-glycerate kinase (at  $5^\circ\text{C}$ ). Both solutions were buffered in 0.2 M Hepes at pH

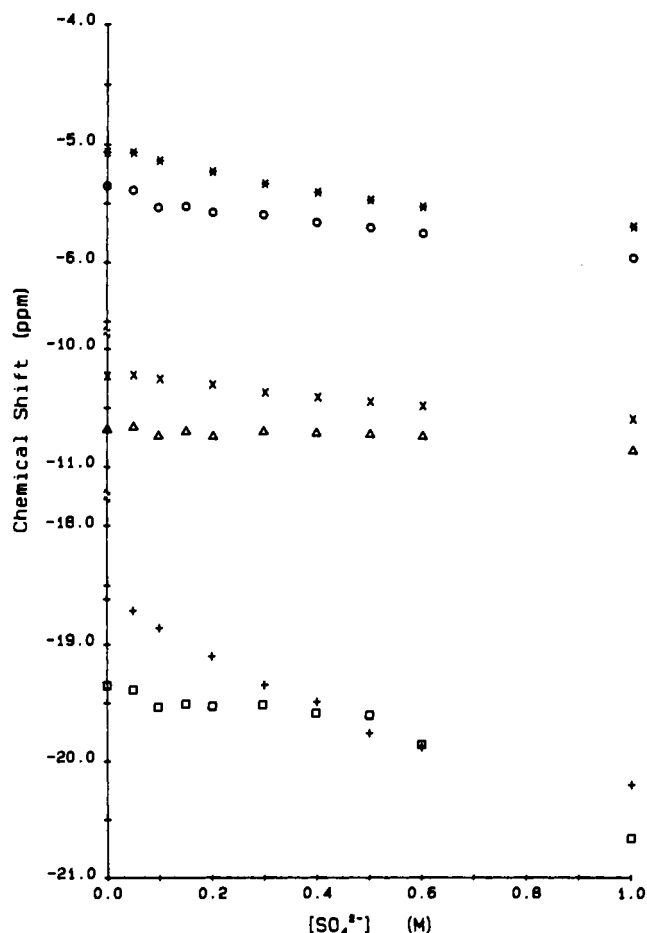


FIGURE 1: Variation of  $^{31}\text{P}$  chemical shifts with sulfate concentration for  $\alpha$ - (x),  $\beta$ - (+), and  $\gamma$ - (\*) P of  $\text{MgATP}$  and for  $\alpha$ - ( $\Delta$ ),  $\beta$ - ( $\square$ ), and  $\gamma$ - ( $\circ$ ) P of  $\text{E-MgATP}$ .  $\text{MgATP}$  sample conditions: 3 mM ATP and 6 mM  $\text{MgCl}_2$  in pH 8.2 0.2 M HEPES buffer with appropriate  $(\text{NH}_4)_2\text{SO}_4$ . NMR parameters: pulse width,  $15\text{ }\mu\text{s}$  ( $\sim 70^\circ$ ); sweep width,  $\pm 2000$  Hz; data size, 4096; line broadening, 2 Hz; number of scans, 300; recycle delay, 3 s. Enzyme samples were kept at  $5^\circ\text{C}$  and started as 1 mL of 3.7 mM ATP, 5.6 mM enzyme, 11 mM  $\text{MgCl}_2$ , and 0.2 M HEPES, pH 8.2. This was titrated with 3.7 M  $(\text{NH}_4)_2\text{SO}_4$  in 0.2 M HEPES, pH 8.2. Enzyme sample NMR parameters: same as above except data size, 2048; line broadening, 40 Hz; number of scans, 500.

8.2. Recalling that the  $^{31}\text{P}$  resonance of  $\beta$ -P (ATP) occurs at  $\sim -21.5$  ppm, the data in Figure 1 show that as a result of progressive increase in sulfate concentration the  $\beta$ -P resonance appears to go through the stages of  $\text{Mg(II)}$  titration (Vasavada et al., 1984) in reverse. Similar effects were also seen with  $\text{MgADP}$  and  $\text{E-MgADP}$  (data not shown). The reduction in the values of  $^{31}\text{P}$ - $^{31}\text{P}$  spin-spin coupling constants of both ADP and ATP by  $\sim 5$  Hz upon  $\text{Mg(II)}$  chelation in free solution is also reversed due to the addition of sulfate (data not shown). For the enzyme-bound complexes, on the basis of previously published dissociation constants (Scopes, 1978a), the fractional concentration of free metal-nucleotide complexes ( $[\text{M}\cdot\text{S}]/[\text{E}\cdot\text{M}\cdot\text{S}]$ ) never exceeded 5%. All these data clearly show that at sufficiently high concentrations of sulfate, the  $^{31}\text{P}$  NMR parameters revert to their values in the absence of  $\text{Mg(II)}$ . Sulfate thus interferes with the interaction of  $\text{Mg(II)}$  with the phosphate groups of ATP and ADP free in solution as well as in their enzyme-bound complexes.<sup>2</sup> Crystallization of

<sup>2</sup> Since  $\text{Mg(II)}$  has affinity for the sulfate ion, albeit weaker than that for the nucleotides, at pH 8.2, the effect of excess sulfate on Free  $\text{MgATP}$  and  $\text{MgADP}$  is anticipated. These measurements are made for the sake of comparison with data on the effect of sulfate on enzyme-bound  $\text{Mg(II)}$ -nucleotide complexes, which is the issue of relevance here.

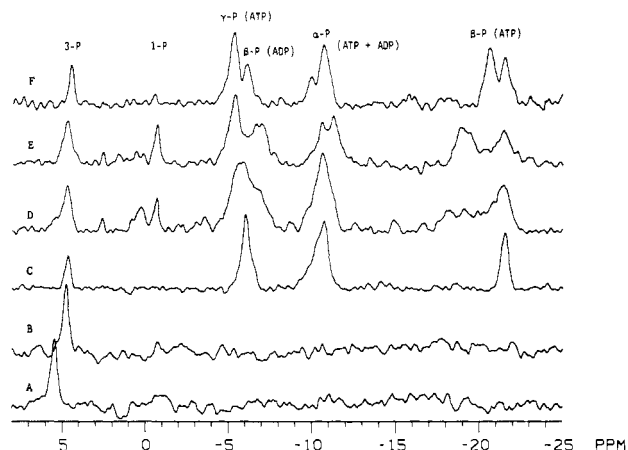


FIGURE 2: Sulfate and Mg(II) effects on a 3-P-glycerate kinase reaction mixture. All samples were at 5 °C in 0.2 M HEPES, pH 8.2. (A) Initial sample of 6.1 mM enzyme and 2.1 mM 3-P-glycerate in 1.2 mL. (B)  $(\text{NH}_4)_2\text{SO}_4$  added to sample A, final concentration 51.1 mM. (C) ATP added to sample B, final concentration 2.1 mM. (D)  $\text{MgCl}_2$  added to sample C, final concentration 2.6 mM [ $\text{Mg}(\text{II})$ :ATP = 1.2:1]. (E)  $\text{MgCl}_2$  added to sample D, final concentration 6.0 mM [ $\text{Mg}(\text{II})$ :ATP = 3:1]. (F) EDTA added to sample E, final concentration 5.9 mM. Additions caused a dilution of enzyme concentration to 5.9 mM in sample F. NMR parameters were the same as in Figure 1 except the pulse width was 12  $\mu\text{s}$  ( $\sim 60^\circ$ ) and the sweep width was  $\pm 2400$  Hz.

3-P-glycerate kinase does not occur until sulfate concentration is greater than  $\sim 2.2$  M. Yet, the chemical shifts indicate that Mg(II) begins dissociating from ATP in the E-MgATP complex at about 0.5 M sulfate. This implies that crystallographic data obtained for the E-MgATP complex will be beset with sulfate interference with proper metal binding. The E-MgADP complex shows appreciably less dissociation of Mg(II) at similar concentrations of sulfate than does the E-MgATP complex. This result correlates well with the relative affinity of the cation to the two complexes (Chapman et al., 1977).

At low concentrations, sulfate has been shown to have some effect on 3-P-glycerate kinase activity and substrate binding (Scopes, 1978b). The spectra in Figure 2 (A and B) show that 50 mM sulfate causes a  $\sim 0.5$  ppm upfield chemical shift of the  $^{31}\text{P}$  resonance of enzyme-bound 3-P-glycerate. (Sulfate, however, does not have any effect on the chemical shift of free 3-P-glycerate.) Addition of ATP to the E-3-P-glycerate (Figure 2C) and later Mg(II) to form the equilibrium mixture (Figure 2D,E) caused negligible shift of the 3-P-glycerate signal.<sup>3</sup> The broad shoulder on the low-field side of this resonance in Figure 2D is assigned to 3-P of 1,3-bis-P-glycerate, the 1-P resonance of which occurs at 0.1 ppm with an apparent splitting. The general features of the spectra in Figure 2D are similar to those in the previous  $^{31}\text{P}$  NMR work (Nageswara Rao et al., 1978), where the shift of enzyme-bound 3-P-glycerate upon the addition of sulfate was noted in the equilibrium mixture. Parts A and B of Figure 2 show that the shift in this resonance is caused exclusively by the addition of sulfate, irrespective of the presence of ATP or Mg(II) on the enzyme. Addition of excess Mg(II) [ $\text{Mg}(\text{II})$ :ATP = 3.0] causes shifts in the resonances of 1,3-bis-P-glycerate, leading to a merging of its 3-P resonance with that of 3-P-glycerate and removing the doubling in the 1-P resonance (see Figure 2E). Figure 2E also displays changes

<sup>3</sup> The spectra shown in Figure 2 were recorded for  $^{31}\text{P}$  chemical shift measurements only. Because of the long relaxation time for the  $^{31}\text{P}$  nucleus in enzyme-bound 3-P-glycerate (Ray & Nageswara Rao, 1988) this resonance is not completely relaxed. Therefore, peak areas in these spectra do not accurately reflect relative concentrations.

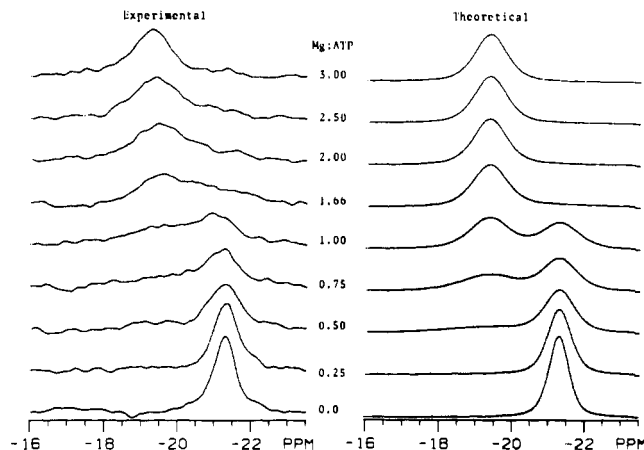


FIGURE 3: Line shape of  $\beta$ -P of ATP in a titration of the E-ATP complex with  $\text{MgCl}_2$  at 5 °C. (A) Experimental curves at varying ratios of Mg(II) to ATP. Sample consisted initially of 5.7 mM enzyme and 3.9 mM ATP and, at the end of the titration, 5.4 mM enzyme and 3.7 mM ATP. NMR parameters were the same as in Figure 1. (B) Simulated spectra for different [ $\text{Mg}(\text{II})$ ]:[ATP] values based on slow exchange with chemical shift positions of  $-19.3$  ppm (E-MgATP) and  $-21.3$  (E-ATP) for both sites (in the absence of exchange) and concentrations of contributing species calculated by using the equilibrium constants (see Appendix for definitions)  $K_1 = 30 \mu\text{M}$ ,  $K_2 = 65 \mu\text{M}$ ,  $K_S = 70 \mu\text{M}$ ,  $K_D = 0.5 \text{ mM}$ ,  $K_2' = 5 \text{ mM}$ ,  $K_S' = 0.5 \text{ mM}$ , and  $K_D' = 0.5 \text{ mM}$ .

in the line shapes of the nucleotide resonances coming from excess Mg(II), and these features are addressed in the next section. Figure 2F shows the effect of removing Mg(II) from the reaction complexes by adding EDTA. The line shape of the  $\beta$ -P (ATP) resonance indicates that all the Mg(II) is not sequestered. However, the significant sharpening of the resonances compared to those in Figure 2E indicates that the reaction is practically stopped. It is interesting that the resonances of 1,3-bis-P-glycerate are virtually unobservable in Figure 2F, indicating a shift in the equilibrium toward E-ATP-3-P-glycerate as the Mg(II) available to the reaction complex is progressively depleted.<sup>4</sup>

**Mg(II) Affinity at the Two ATP Sites.** It has been recognized for some time that there are two ATP-binding sites on 3-P-glycerate kinase (Larsson-Raznikiewicz & Schierbeck, 1977; Scopes, 1978a), and previous  $^{31}\text{P}$  NMR results clearly showed that these two sites have markedly different affinities for Mg(II) (Nageswara Rao et al., 1978). The line shapes of the  $\beta$ -P (ATP) resonance that occurs in the region  $-18$  to  $-22$  ppm in Figures 2D are indicative of this disparity between the two sites. For the design and analysis of relaxation measurements in the presence of activating paramagnetic cations, reliable estimates of the concentrations of the various species of enzyme-bound complexes with and without the cation are required. The line shape of  $\beta$ -P (ATP) and the chemical shift of  $\gamma$ -P (ATP) exhibit easily measurable sensitivity to Mg(II) chelation and may, therefore, be used as an experimental basis for such estimates. Figure 3A shows the effect of varying Mg(II) concentration on the line shape of the  $\beta$ -P (ATP) signal. Figure 4 shows the effect on the chemical shift of  $\gamma$ -P (ATP) in the same experiment. The  $\beta$ -P (ATP) signal in Figure 3A represents two signals in slow exchange (chemical shift difference is large compared to exchange rate). These two signals are located (in the absence of exchange) at the chemical shift positions of  $-19.3$  ppm

<sup>4</sup>  $^{31}\text{P}$  NMR spectra recorded with EDTA concentrations less than that used for Figure 2F do show 1-P resonances arising from 1,3-bis-P-glycerate. The intensity of this signal is intermediate between that in Figure 2E,F.

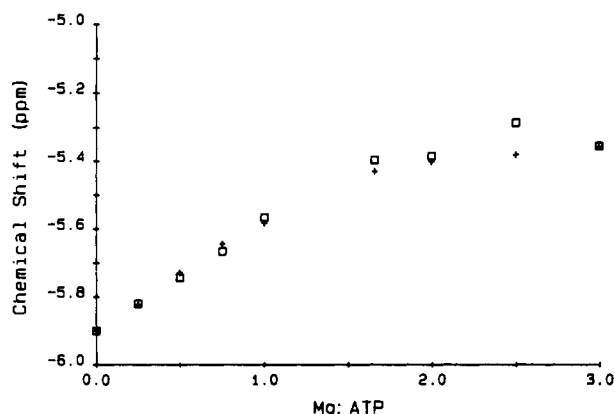


FIGURE 4: Observed (□) and calculated (+) variation in the chemical shift of  $\gamma$ -P (ATP) in the E-ATP complex at 5 °C with  $[\text{Mg(II)}]:[\text{ATP}]$  for the sample described in Figure 3. Theoretical values are based on fast exchange with the concentrations of contributing species calculated for Figure 3B and chemical shifts of -5.9 ppm in the absence of Mg(II) and -5.33 ppm with Mg(II) chelated to ATP at either of the two binding sites (in the absence of exchange).

(E-MgATP) and -21.3 ppm (E-ATP) irrespective of the binding site. The chemical shifts of  $\gamma$ -P (ATP) plotted in Figure 4, on the other hand, represent an average of the chemical shifts of  $\gamma$ -P of E-ATP and E-MgATP (-5.9 and -5.33 ppm, respectively, in the absence of exchange) weighted by their respective concentrations because these resonances are in fast exchange.

In order to compute the concentrations required for simulating the line shape of  $\beta$ -P (ATP) in Figure 3A and the average chemical shift of  $\gamma$ -P (ATP) in Figure 4, a model of substrate binding was devised in which it was assumed that each site was independent of the other. The details of the model are described in the Appendix. In computing the spectra shown in Figure 3B, line widths of the observed  $\beta$ -P resonances were measured at each concentration of Mg(II) and used as the widths of the corresponding simulated lines. Intensities were adjusted to give areas corresponding to the calculated concentrations of E-MgATP and E-ATP for each value of Mg(II) used. Various combinations of values for the independent equilibrium constants were tried, starting with values suggested by Scopes (1978a), and the best fit was selected by visual comparison of the simulated spectrum to the observed spectrum. Figure 3B and the theoretical curve in Figure 4 show the results for the best case found. The equilibrium constants were  $K_1 = 30 \mu\text{M}$  for the binding of Mg(II) with ATP;  $K_2 = 65 \mu\text{M}$ ,  $K_S = 70 \mu\text{M}$ , and  $K_D = 0.5 \text{ mM}$  for the enzyme active site; and  $K_2' = 5 \text{ mM}$ ,  $K_S' = 0.5 \text{ mM}$ , and  $K_D' = 0.5 \text{ mM}$  for the second site. (See the Appendix for the definitions of  $K_2$ ,  $K_S$ , and  $K_D$ .) The overall agreement between the simulated and observed line shapes of  $\beta$ -P in Figure 3 and that between the calculated and observed chemical shifts of  $\gamma$ -P in Figure 4 is quite good,<sup>5</sup> suggesting that the independent-binding model is reasonable for this case, although it was initially chosen for reasons of tractability and simplicity.

**pH Dependence of  $^{31}\text{P}$  Chemical Shifts of Enzyme-Bound Complexes.**  $^{31}\text{P}$  chemical shift measurements (data not shown) between pH 4.5 and 9.0 for free 3-P-glycerate and between pH 6.2 and 9.0 for 3-P-glycerate in the E-MgADP-3-P-

glycerate complex showed that while free 3-P-glycerate titrates in this range with  $\text{p}K_a \approx 7.0$ , chemical shift for bound 3-P-glycerate remains unchanged, indicating that the bound 3-P-glycerate is in an environment substantially different from that in bulk solution. Likewise, the chemical shift of the  $\beta$ -P of MgADP in the E-MgADP-3-P-glycerate complex is unchanged over the same pH range, while the  $\beta$ -P of free MgADP titrates with  $\text{p}K_a \approx 6.0$ . Similarly, none of the chemical shifts of the three phosphate groups of ATP in the E-MgATP complex changed in the range pH 6.4–9.0. In every case, the substrate appears to be sequestered from bulk solution.

## DISCUSSION

Most of the X-ray crystallographic studies of 3-P-glycerate kinase [e.g., Bryant et al. (1974) and Watson et al. (1982)] employed ammonium sulfate crystallization, which is by far the most common method. These crystals contained sulfate ion concentrations in excess of 2 M. There is evidence from NMR (Nageswara Rao et al., 1978) and kinetic (Scopes, 1978a) measurements that sulfate ion interacts with the substrates at the active site of this enzyme. The question then arises as to the effect of the high sulfate ion concentrations on the X-ray structural data of the enzyme-substrate complexes in general, and, in particular, with regard to the location of the cation Mg(II) in the vicinity of the phosphate groups of the enzyme-bound nucleotides. The magnetic resonance methods (NMR and ESR) are appropriate to address this question as the sample conditions for these do not require the presence of the sulfate, and, indeed, measurements may be made with and without sulfate. The  $^{31}\text{P}$  NMR results presented in this paper on the effect of sulfate on the chemical shifts and spin-spin coupling constants of free<sup>2</sup> and enzyme-bound MgATP and MgADP clearly indicate that the large sulfate concentrations are most likely to alter the structure of the Mg(II)-nucleotide complexes of the enzyme, especially that of E-MgATP. These data serve as a prelude to NMR measurements of the distances between the  $^{31}\text{P}$  nuclei in the enzyme-bound nucleotides from substituent paramagnetic cations such as Mn(II) and Co(II) to be presented in the following paper (Ray & Nageswara Rao, 1988).

Another question pertinent to the analysis of relaxation data on enzyme-bound cation-nucleotide complexes in the presence of paramagnetic cations (Ray & Nageswara Rao, 1988) regards the relative affinities of the cation for ATP bound to the enzyme at the two sites. The sensitivity of the  $\beta$ -P and  $\gamma$ -P resonances of ATP, especially the former, to cation chelation to ATP is well-known and has been used to determine the dissociation rates of cations bound to ATP (Vasavada et al., 1983) by simulations of the line shape of the  $\beta$ -P (ATP) resonance in the presence of varying concentrations of Mg(II). The analysis presented in this paper is based on an independent-binding model for the two sites, which is the simplest way to reduce the contribution of a vast number of equilibria to a limited number of parameters that determine the observed NMR line shapes and chemical shifts. An iterative fit of the calculated and observed spectra showed that ATP binds about 7-fold weaker and MgATP about 70-fold weaker at the secondary enzyme site compared to binding at the catalytic site. The agreement between the calculated and observed line shapes and chemical shifts is quite close, indicating that the independent-binding model may actually be appropriate to describe ATP binding in the presence of Mg(II) at the two sites of 3-P-glycerate kinase.

$^{31}\text{P}$  chemical shifts of enzyme-bound MgADP, MgATP, and 3-P-glycerate show no discernible variation in the pH range 6.2–9.0. Since all these substrates contain titratable phosphate

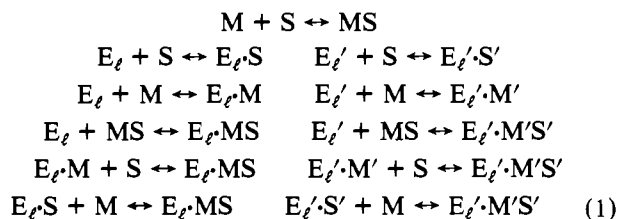
<sup>5</sup> There is an apparent deviation between experimental and calculated line shapes in Figure 3 in the region of  $[\text{Mg}]:[\text{ATP}] \approx 1.0$ . However, for the same range the calculated  $\gamma$ -P chemical shifts agree quite well with experiment in Figure 4, indicating that the deviation in Figure 3 is likely to be primarily due to the line shape rather than an incorrect value of the calculated concentration.

groups in this pH range in free solution, this result suggests that in the enzyme-bound complexes these phosphate moieties are well sequestered from bulk solution. It may be tempting to interpret this result to conclude upon the ionic state of the substrates in the enzyme-bound complexes. However, such a conclusion will be based on the implicit but questionable assumption that pH dependence of the chemical shifts of substrate nuclei in the enzyme-bound complexes are determined by the same factors as those in free solution (Nageswara Rao, 1984).

## APPENDIX

**Metal-Nucleotide Binding at Two Independent Sites.** There are 19 different species as follows: E, S, M, and MS; E·S, E·S', E·M, E·M', E·MS, and E·M'S'; E·S·S', E·M·M', E·M·S', E·S·M', E·MS·S', E·S·M'S', E·M·M'S', E·MS·M', and E·MS·M'S'. E, S, and M denote enzyme, substrate, and metal, respectively, and the prime denotes binding to the secondary site.

Independence of the binding sites implies that any equilibrium involving one site has the same equilibrium constant regardless of the occupancy of the other site. Thus, e.g.,  $K_S = [E][S]/[E·S] = [E·S']/[E·S·S'] = [E·M']/[E·S·M'] = [E·M'S']/[E·S·M'S']$  and so forth throughout the various related equilibria. The following pseudoequilibria can then be defined



where

$$\begin{array}{l} E_\ell = E + E·S' + E·M' + E·M'S' \\ E'_\ell = E + E·S + E·M + E·MS \end{array} \quad (2)$$

By analogy to previous work (Reed et al., 1970), equilibrium constants can be defined as follows:

$$\begin{array}{l} K_1 = [M][S]/[MS] \\ K_2 = [E_\ell][MS]/[E_\ell \cdot MS] \\ K_2' = [E'_\ell][MS]/[E'_\ell \cdot M'S'] \\ K_S = [E_\ell][S]/[E_\ell \cdot S] \quad K_S' = [E'_\ell][S]/[E'_\ell \cdot S'] \\ K_D = [E_\ell][M]/[E_\ell \cdot M] \quad K_D' = [E'_\ell][M]/[E'_\ell \cdot M'] \\ K_3 = [E_\ell \cdot M][S]/[E_\ell \cdot MS] \\ K_3' = [E'_\ell \cdot M'][S]/[E'_\ell \cdot M'S'] \\ K_A = [E_\ell \cdot S][M]/[E_\ell \cdot MS] \\ K_A' = [E'_\ell \cdot S'][M]/[E'_\ell \cdot M'S'] \end{array} \quad (3)$$

Note that

$$\begin{array}{ll} K_3 = K_1 K_2 / K_D & K_3' = K_1 K_2' / K_D' \\ K_A = K_1 K_2 / K_S & K_A' = K_1 K_2' / K_S' \end{array} \quad (4)$$

The mass balance equations are

$$\begin{array}{l} [S]_T = [S] + [MS] + [E_\ell \cdot S] + [E'_\ell \cdot S'] + [E_\ell \cdot MS] + [E'_\ell \cdot M'S'] \\ [M]_T = [M] + [MS] + [E_\ell \cdot M] + [E'_\ell \cdot M'] + [E_\ell \cdot MS] + [E'_\ell \cdot M'S'] \\ [E]_T = [E_\ell] + [E_\ell \cdot S] + [E_\ell \cdot M] + [E_\ell \cdot MS] \\ [E']_T = [E'_\ell] + [E'_\ell \cdot S'] + [E'_\ell \cdot M'] + [E'_\ell \cdot M'S'] \end{array} \quad (5)$$

Iterative computations of the concentrations of the relevant species now reduces to a straightforward extension of the algorithm of Reed et al. (1970). For the specific problem of simulating the line shape of the  $^{31}\text{P}$  resonance  $\beta$ -P of ATP bound at the two sites on 3-P-glycerate kinase in the presence of Mg(II) and undergoing slow exchange, the quantities of interest are  $[E_\ell \cdot S + E'_\ell \cdot S']$  and  $[E_\ell \cdot MS + E'_\ell \cdot M'S']$ . The same quantities are used to compute the average chemical shift of the corresponding  $\gamma$ -P (ATP) resonances in fast exchange.

**Registry No.** ATP, 56-65-5; MgATP, 1476-84-2;  $\text{SO}_4^{2-}$ , 14808-79-8; Mg, 7439-95-4.

## REFERENCES

- Adams, B., & Pain, R. H. (1986) *FEBS Lett.* **196**, 361–364.  
 Adams, B., Burgess, R. J., & Pain, R. H. (1985) *Eur. J. Biochem.* **152**, 715–720.  
 Banks, R. D., Blake, C. C. F., Evans, P. R., Haser, R. Rice, D. W., Hardy, G. W., Merrett, M., & Phillips, A. W. (1979) *Nature (London)* **279**, 773–777.  
 Blake, C. C. F., & Rice, D. W. (1981) *Philos. Trans. R. Soc. London, B* **293**, 93–104.  
 Bryant, T. N., Watson, H. C., & Wendell, P. L. (1974) *Nature (London)* **247**, 14–17.  
 Chapman, B. E., O'Sullivan, W. J., Scopes, R. K., & Reed, G. H. (1977) *Biochemistry* **16**, 1005–1010.  
 Fifis, T., & Scopes, R. K. (1978) *Biochem. J.* **175**, 311–319.  
 Larsson-Raznikiewicz, M., & Schierbeck, B. (1977) *Biochim. Biophys. Acta* **481**, 283–287.  
 Mas, M. T., Resplandor, Z. E., & Riggs, A. H. (1987) *Biochemistry* **26**, 5369–5377.  
 Moore, J. M., & Reed, G. H. (1985) *Biochemistry* **24**, 5328–5333.  
 Nageswara Rao, B. D. (1984) in *Phosphorus-31 NMR: Principles and Applications* (Gorenstein, D. G., Ed.) pp 57–103, Academic, New York.  
 Nageswara Rao, B. D., Cohn, M., & Scopes, R. K. (1978) *J. Biol. Chem.* **253**, 8056–8060.  
 Pickover, C. A., McKay, D. B., Engleman, D. M., & Steitz, T. A. (1979) *J. Biol. Chem.* **254**, 11323–11329.  
 Ray, B. D., & Nageswara Rao, B. D. (1988) *Biochemistry* (following paper in this issue).  
 Reed, G. H., Cohn, M., & O'Sullivan, W. J. (1970) *J. Biol. Chem.* **245**, 6547–6552.  
 Rice, D. W., & Blake, C. C. F. (1984) *J. Mol. Biol.* **175**, 219–223.  
 Roustau, C., Fattoum, A., Jeanneau, R., & Pradel, L.-A. (1980) *Biochemistry* **19**, 5168–5175.  
 Scheffler, J. E., & Cohn, M. (1986) *Biochemistry* **25**, 3788–3796.  
 Scopes, R. K. (1969) *Biochem. J.* **113**, 551–554.  
 Scopes, R. K. (1971) *Biochem. J.* **122**, 89–92.  
 Scopes, R. K. (1973) *Enzymes (3rd Ed.)* **8**, 335–351.  
 Scopes, R. K. (1978a) *Eur. J. Biochem.* **91**, 119–129.  
 Scopes, R. K. (1978b) *Eur. J. Biochem.* **85**, 503–516.  
 Vasavada, K. V., Ray, B. D., & Nageswara Rao, B. D. (1984) *J. Inorg. Biochem.* **21**, 323–335.  
 Watson, H. C., Walker, N. P. C., Shaw, P. J., Bryant, T. N., Wendell, P. L., Fothergill, L. A., Perkins, R. E., Conroy, S. C., Dobson, M. J., Tuite, M. F., Kingsman, A. J., & Kingsman, S. M. (1982) *EMBO J.* **12**, 1635–1640.  
 Wilson, C. A. B., Hardman, N., Fothergill-Gilmore, L. A., Gamblin, S. J., & Watson, H. C. (1987) *Biochem. J.* **241**, 609–614.